AP1000 Reactor Design
Nuclear Reactor Technology (SH2702 VT23)

Team 53
Amit Hasan Arpon
Hadiza Ahmad Abubakar

March 6, 2023

Contents

1 Introduction

This report focuses on the AP1000 PWR reactor and includes a broad description of the reactor, its features, operating principles, and thermal-hydraulic properties. The report is divided into six tasks, with the first three tasks of the project focusing on AP1000 literature research and the last three on calculations to determine the fundamental design characteristics of the reactor core.

2 Task 1: General design specification of AP1000

2.1 AP1000 general describtion

Westinghouse Electric Company's AP1000 is a generation III+ pressurized water reactor (PWR) with a thermal output of 3,400 MWth. The AP1000 design incorporates proven technology and passive safety features in an effort to provide a safe, easy-to-maintain, and dependable power plant. The AP1000 design incorporates streamlined systems to improve operability while minimizing components, maintenance, and surveillance requirements, hence reducing the nuclear power plant's capital and operational costs.

The AP1000 was designed with environmental concerns in mind. [1] The operational discharges, and exposure of workers to radiation, radiation, and hazardous waste have been minimized. The general design specifications for the AP1000 comprise the reactor core and fuel design, reactor vessel, primary loop, and balance of plant (BoP).

2.2 Reactor core and fuel design

The core of the reactor houses fuel assemblies, internal structural components, and control elements. The fuel assemblies are 157, 426.7 cm long, 17×17. The internal structure directs the flow of coolant (light water) through the fuel assemblies, within and out of the core, at a pressure of 17.1 MPa. The core utilizes the Westinghouse ROBUST design with a 15% margin to nucleate boiling (DNB), Zirlo grids as cladding, and removable top nozzles. [2]

The core is made up of three radial zones with varying enrichments; the fuel enrichment ranges from 2.35 w% to 4.8 w% ^{235}U. The core is designed for an 18-month fuel cycle with a capacity factor of 93% and region average discharge burnups of up to 60000 MWd/t. [1]
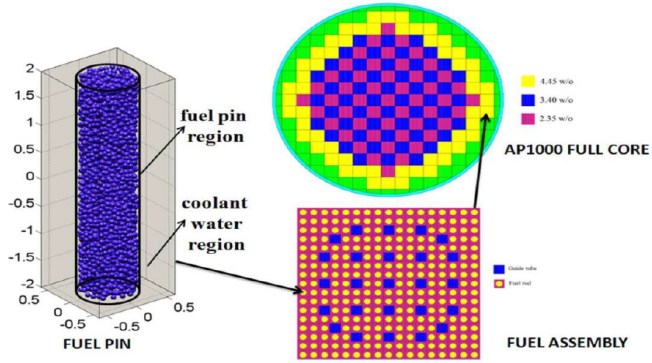
Figure 1: Schematic for the AP1000 reactor core, fuel assembly and fuel pin. [3]

As shown in Fig.1, each fuel assembly in the core has 24 spots reserved for guide tubes that house control elements, with the central position remaining vacant for instrumentation. Fuel rod positions are occasionally substituted with burnable poisons to improve reactivity control owing to fuel burnup. [3]

2.3   Reactor vessel

The reactor vessel as seen in Fig.2 is constructed with thick walls that enclose the fuel assemblies, internals, and coolant. The vessel is a high-pressure containment barrier that is cylindrical in shape with a hemispherical bottom and a removable top head. The vessel is made of low-alloy steel and used to hold in the core. The vessel is 12 m long and 3.988 m in diameter, with a design life of 60 years under 17.1 MPa and 343°C under operational conditions. [2]
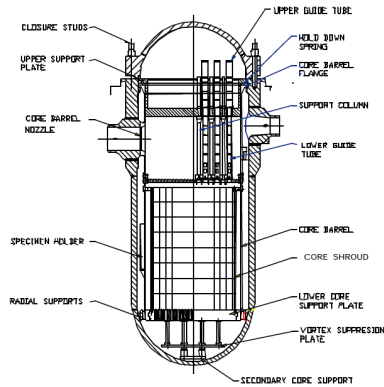

Figure 2: AP1000 reactor vessel. [3]

As a safety measure, the vessel eliminates the potential of a coolant loss accident caused by leakage from the reactor vessel, which might result in core exposure.

2.4 Reactor primary loop

The system consists of a steam generator (SG), two reactor coolant pumps installed directly onto the SG, two heat transfer circuits with a single hot leg (transporting reactor coolant to SG) and two cold legs (transporting reactor coolant back to reactor vessel). By eliminating the piping between the SG and the pump, the loop pressure drop is decreased, and the system is simplified. The two cold leg lines in the loop are bent to provide a low-resistance flow path and mobility to handle the difference in expansion between the hot and cold leg pipes. [2]

The SG design is based on the Delta 75 and Delta 95 proven designs and includes enhancements such as nickel-chromium-iron Alloy 690 thermally treated tubes, improved anti-vibration bars, upgraded moisture separators and enhanced maintenance features. [1] The lack of seals on the reactor coolant canned-motor pumps eliminates the risk of seal failure LOCA, which considerably improves safety and reduces pump maintenance. Based on proven technology, the large pressurizer with a volume of 59.5 m^3 reduces challenges during transients by increasing operational margins, resulting in a more dependable plant with fewer reactor trips. [1]

The primary loop configuration and material selection yield sufficiently low pipe stresses to meet leak-before-break standards for the primary loop and auxiliary lines. The system structure simplifies in-service inspections and enhances maintenance accessibility. [1]
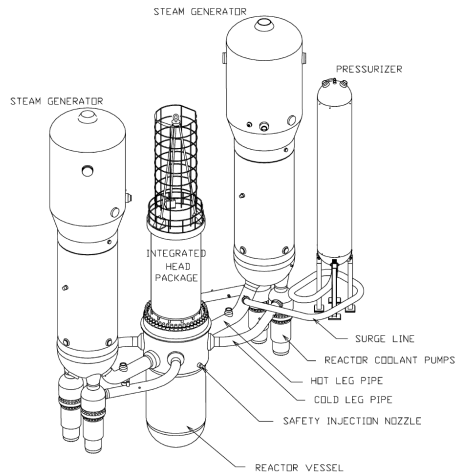

Figure 3: AP1000 primary loop. [4]

2.5 Balance of plant (BoP)

The balance of plant (BoP) is the sum of supporting and auxiliary systems that are required to deliver energy, other than the generating unit (the reactor and steam generators) as shown in Fig.4. [5] The reactor produces power and generates electricity through the BoP systems. BoP contains several components and sub-systems, such as titanium condensers, turbines, motor-driven feedwater pumps, feedwater sub-systems, refuel water storage tank in the containment building, and safety-related diesel engines etc.
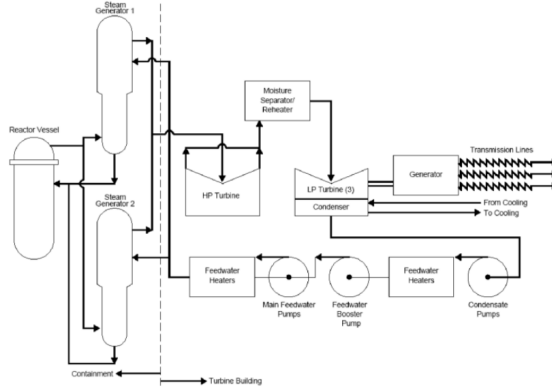

Figure 4: Simplified balance of plant for AP1000. [6]

3 Task 2: AP1000 Operational principles

3.1 Normal operation

Normal operations of the AP1000 cover six (6) anticipated modes of operation with respect to reactivity (multiplication factor), thermal power, average coolant temperature, and vessel closure, [7] as shown in Table 1.

Depending on the mode of operation, the condition of the reactor at that state changes. Therefore, the following describes the conditions involved with power, startup and shutdown operations.

- **Power Operation**
  In power operating mode, positive reactivity is introduced and the reactor generates power via the SGs, turbine, condenser, and main feed systems. The steam from the steam generator (SG) is delivered to the high turbine (HT) by the mainstream system (MSS). Following expansion in the HT, the steam is reheated by two moisture separator reheaters (MSRs) before being admitted to the three Low-pressure turbines (LPT). A portion of the steam

Table 1: AP1000 modes of normal operation.

Mode		Reactivity Condition (K_{eff})	% Rated Thermal Power	Average Coolant Temperature
1	Power operation	≥0.99	> 5	N/A
2	Startup	≥0.99	≤5	N/A
3	Hot standby	<0.99	N/A	>215.6°C
4	Safe shutdown	<0.99	N/A	≤215.6°C
5	Cold shutdown	<0.99	N/A	≤93.3°C
6	Refuelling	N/A	N/A	N/A

from the HPT and LPT is extracted for seven stages of feedwater heating. Meanwhile, the main condenser condenses and deaerates the LPT's exhaust steam, and the circulating water system removes the heat rejected by the condenser. The condensate is then fed to the two SGs via four stages of closed low-pressure feedwater heaters, an open deaerating heater, and two stages of high-pressure feedwater heaters. [7]

- **Startup**
  A start-up mode includes activities that transition a power plant from hot standby to power operation and vice versa. Once the Reactor coolant system has been heated but is still subcritical, the Chemical and Volume Control System (CSV) eliminates boron from the Reactor coolant system (RCS), thereby improving reactivity and power by modifying the control rods. Until the control of feedwater is automatically transferred from the startup feedwater control valves to the main feedwater control valves, feedwater continues to be provided through the startup feedwater control valves as power grows. When thermal power (excluding decay heat) exceeds 5% of the thermal power rating, the reactor enters power operation mode. [7]

- **Safe shutdown**
  During plant heat-ups and cooldowns, the safe shutdown mode is activated, which entails keeping the reactor subcritical at an average coolant temperature between 215.6 and 93.3 degrees and maintaining an appropriate coolant inventory and core cooling. During safe shutdown operation, the SGs and the normal residual heat removal system (RNS) in normal operations eliminate decay heat. In post-failure situations, however, the passive residual heat removal system (PRHR) is capable of achieving safe shutdown conditions within 36 hours by automatically rejecting core decay heat from the RCS to the in-containment refuelling water storage tank (IRWST). Approximately two hours after the PRHR heat transfer system is initiated, the IRWST water reaches the saturation point and begins to steam into the confinement atmosphere. There, it condenses on the passive containment cooling system-cooled steel containment shell and is collected via a gutter

arrangement at multiple elevations of the containment vessel before being drained back into the IRWST. This method preserves the PRHR HX heat sink. [7]

3.2 Ractivity control method

The primary purpose of core control is to manage core reactivity and power distributions simultaneously. In AP1000, there are two reactivity control systems, one of which consists of two independent, movable rod control cluster assembly (RCCA) groups that provide core control, and the other of which consists of soluble boric acid in the RCS.
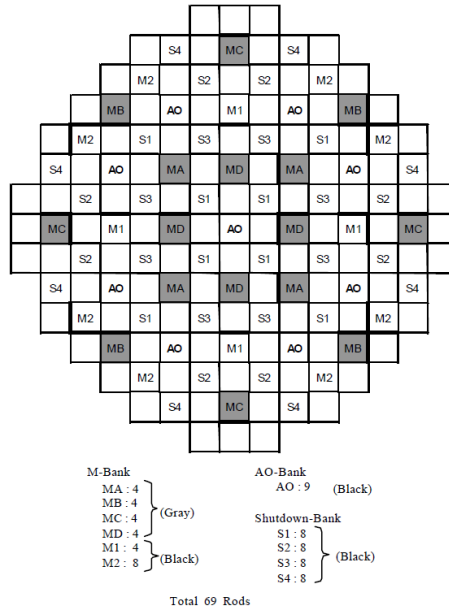

Figure 5: Rod control cluster assembly (RCCA) configuration. [8]

Fig. 5 displays the AP1000's typical RCCA configuration, in which 69 RCCAs are placed in a checkerboard pattern and have the following configurations:

- M-Bank consisting of normal black rods and reduced worth grey rods

- AO- Bank (axial offset) consist of just Black rods

- S- Bank (shutdown) consist of just Black rods

The two RCCA groups are employed to manage reactivity/temperature utilizing the M-banks and manage the axial power distribution with the AO banks. This control strategy is known as MSHIM (Mechanical Shim) and it eliminates

the need for Chemical Shim modifications during power movements, such as load following. [8]

In contrast, the boron system can compensate for xenon burnout reactivity fluctuations and keep the reactor in a cold shutdown state. Additionally, the boron system accommodates fluctuations in reactivity caused by fuel depletion. Mechanical and chemical shim control systems that meet the design requirements provide backup and emergency shutdown provisions. [8]

3.3   Load operation scenarios

The AP1000 is designed to offer extended base load and load following capabilities. Using the RCCA, it is possible to operate at base load while regularly altering the boron concentration as the fuel depletes to reposition the M-banks and permit a periodic replacement of the grey rod M-bank insertion sequence.

The design can also execute load follow operation for up to 95 % of cycle life by using the MSHIM control method, granted that power is automated due to the absence of boron concentration changes and the large reduction in daily effluent to be treated.

The following daily load follow change transients can be handled by AP1000 [9]:

- Power ramps from 100% to 50% in 2 hours

- Power remains at 50% for 2 to 10 hours

- Power ramps back up to 100% in 2 hours

- Power remains at 100% for the remainder of the 24-hour cycle

During daily load follow and load regulation transients, these capabilities are achieved without a reactor trip or steam dump actuation. This is possible because the system is designed to restore the average coolant temperature within the established temperature band of the above transient changes. Additionally, within the prescribed insertion limitations, manual control of either the power M banks or the AO bank is accomplished. [9]

3.4   Auxillary system

The auxiliary systems consist of non-electrical and non-HVAC defence in-depth safety systems, water systems and other support systems. There are several auxiliary systems in AP1000, however, the following operational principles are quite unique:

- **The Chemical and Volume Control System (CVS)**
  CVS is made up of numerous heat exchangers, demineralizes, pumps, and instrumentation, to mention a few, and it works together to control Reactor Coolant System chemistry, purity, and inventory for normal plant operations.

- **Normal residual heat removal system (RNS)**
  The RNS performs both normal plant functions and accident functions. In normal operation, the RHR system is used to remove decay heat from the core and bring the reactor coolant temperature down to (93.3°C) until the plant is restarted. During the injection and recirculation phases of a coolant loss event, it also functions as part of the emergency core cooling system. It is also utilized to transport refuelling water before and after refuelling operations between the refuelling water storage tank and the refuelling cavity. [10]

- **The Spent fuel pool cooling system**
  The spent fuel pool cooling system is intended to remove decay heat from stored fuel assemblies by removing heat from the water in the spent fuel pool. This is accomplished by pumping hot water from the fuel pool through a heat exchanger and then returning cooler water to the pool. The clarity and purification of water are supplementary functions of this device. [2]

4 Task 3: Safety features of AP1000

4.1 General principles of AP1000 reactor safety

The fundamental safety objective is to protect people and the environment from the harmful effects of ionizing radiation. [11] This includes ensuring that the danger added by technology is affordable and that the discharge of fission products is avoided. To do so, it is important to establish and carry out the engineering methods dedicated to achieving the aforementioned goal.

The specific safety functions that must be accomplished to assure the general safety objective include:

- The safety function associated with reactivity control includes subcriticality. It is used and developed as the design basis for reactivity control systems such as control rod systems, reactor protection systems, and safety injection. In an emergency, it necessitates testing the ability to scram the reactor.

- Heat extraction is a safety function that is concerned with extracting heat from the core. It is used and developed as the foundation for systems designed to do so under any operational condition, such as emergency core cooling. It generates the requirement to check the capabilities of doing so in an emergency operation.

- Radioactivity confinement is a radioactivity control safety function. It is used and developed as the foundation for the design of systems that deal with containment integrity and radiation extraction, such as containment building systems. It creates the necessity to check the availability of such systems during an emergency operation.

4.2 AP1000 engineered and protection safety features

The AP1000 employs passive Class I safety systems and features to prevent accidents. The benefit of adopting passive safety systems is that long-term accident mitigation is maintained without the need for operator intervention or the use of off-site or on-site AC power. The AP1000 has various safety features, including the Passive Core Cooling System (PXS) and Passive Containment Cooling System (PCCS), both of which have unique features worth mentioning.

- Passive Core Cooling System (PXS)

  1. Two core makeup tanks (CMTs) supply reasonably high-flow borated water over an extended period of time and at any pressure. If an inventory is lost, the CMT subsystem is a passive, safety-related subsystem that injects water into the RCS. To displace the cold injection water, steam is provided to the CMT as seen in Fig. 6.

  2. After the system pressure drops below 4.83 MPa, two pressurized accumulators (ACCs) feed high-flow borated water to the reactor vessel in a short time interval.

  3. After system pressure declines to approach containment pressure, an in-containment refuelling water storage tank (IRWST) delivers low-flow borated water for longer. IRWST/gravity injection floods the refuelling cavity for regular refuelling, floods the confinement postLOCA to establish long-term RCS cooling, and supports PRHR-HXs operation.

  4. A PRHRS with C-shape tube HX inside the IRWST passively removes energy through a natural circulation path between the pressurizer-side hot leg and the steam generator outlet plenum. It has one PRHRHX, valves, pipes, and instrumentation. The IRWST heat sinks high-pressure natural coolant circulation for core cooling.

  5. Two trains of depressurization valves, the first three from the pressurizer and the fourth from hot legs—make up the automated depressurization system (ADS). IRWST heat sinks steam from the first three stages. The fourth-stage valve vents water, steam, or a two-phase mixture to the containment. These valves open sequentially to manage primary system depressurization during LOCA.

  6. The primary system's discharge and containment steam condense in a recirculation sump. After depressurizing the primary system and increasing the gravity head, it allows recirculation water injection. [12]

- Passive Containment Cooling System (PCCS)
  The major goal of PCCS (Fig.7) is to minimize the containment temperature and pressure after the LOCA so that the design pressure does not exceed (0.40 MPa). It can also serve as the ultimate heat sink in an accident. For 72 hours, the steel containment tank provides a heat transfer surface that removes heat from the containment and transmits it to the atmosphere. The

continuous natural circulation of air removes heat from the containment tank. During an accident, water evaporation augmented air cooling, and water drains by gravity from the PCCS gravity drain water tank positioned on top of the containment shield building. [12]
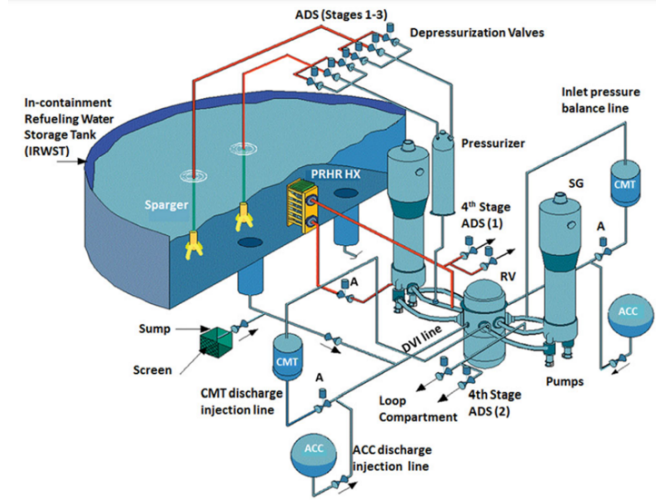

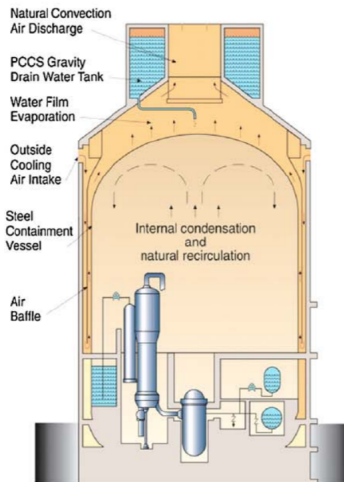Figure 6: AP1000 Passive core cooling system (PXS). [13]

Figure 7: AP1000 Passive containment cooling system (PCCS). [14]

4.3 AP1000 Probabilistic risk analysis

Part 52 of the 10 Code of Federal Regulations requires that a probabilistic risk assessment (PRA) be submitted as a part of an application for design certification. So, Westinghouse committed to the early application of probabilistic analysis techniques in the AP1000 design process. [15]

Table 19.59-17			
COMPARISON OF AP1000 PRA RESULTS TO RISK GOALS			
Plant/Goal	**Core Damage Frequency**	**Large Release Frequency**	**Containment Success Probability**
Current PWR[(1)]	6.7E-05	5.3E-06	92%
NRC Safety Goal	1E-04	1E-06	90%
AP600	1.7E-07	1.8E-08	89%
AP1000	2.41E-07	1.95E-08	92%

Figure 8: AP1000 Probabilistic risk analysis result. [16]

These frequencies are at least two orders of magnitude lower than those of a typical pressurized water reactor installation as seen in Table 4.3 This reduction in risk is the result of a number of plant design elements, with the greatest reduction being from highly dependable and redundant passive safety-related systems that influence both at-power and shutdown hazards. These passive systems are significantly less reliant on operator action and support systems than plant systems in currently operational facilities. [15]

5 Task 4: Calculation of core parameters

5.1 Introduction

AP1000 key core parameters were retrieved from [2,17,18] and tabulated in Table 2. Using the data from Table 2 the following average channel and hot channel thermal-hydraulic characteristics were calculated and the results are presented in subsection 5.3.

- Axial pressure drop distribution

- Axial coolant enthalpy distribution

- Axial coolant temperature distribution

- Flow characteristic of the core, in relationship to the total pressure drop $(-\Delta p_{\text{tot}})$ as a function of mass flux G (varying from 1% to 150%), for core power equal to 0%, 50%, 100% and 150% of the nominal power.

Table 2: AP1000 core parameters.

Core Parameters	Values
The coefficient for the total core heat output	**1.05**
Total core heat output	3400 (MWth)
Total heat output in fuel pellets	3213 (MWth)
Nominal system pressure	15.513 (MPa)
Total core mass flow rate	14300 (kg/s)
Effective fuel cooling mass flow rate	13585 (kg/s)
Number of fuel assemblies	157 (square lattice)
Active fuel height	4.267 (m)
Lattice pitch	12.6 (mm)
Number of fuel rods per assembly	264 rods
Outside fuel rod diameter	9.5 (mm)
Clad thickness	0.57 (mm)
Fuel pellet diameter	8.19 (mm)
Number of spacers grids	10 spacers
Clad roughness	0.0025 (mm)

5.2 Methods

In these calculations, the spatial core power distribution of AP1000 is assumed to be as in Eq.(1)

$$q'(r, z) = q'_0 J_0 \left(\frac{2.405r}{\tilde{R}} \right) \cos \left(\frac{\pi z}{\tilde{H}} \right) \tag{1}$$

where q'_0 is the power at the core centre r = z = 0, J_0 is the Bessel function of the first kind and zero-order and $\tilde{R}, \tilde{H}$ are the extrapolated radius and the extrapolated height of the core, respectively.
The reflected core was assumed to be: $R/\tilde{R} = H/\tilde{H} = 5/6$

The total reactor power used in these calculations was the total core heat output of AP1000 multiplied by a coefficient (**1.05**) (see Table 2).

To simplify the calculations, total power is assigned to each fuel rod, and the rod is divided into 100 cells axially to calculate the core parameters at each cell. When the peaking factors were calculated using Eqs. (2)-(3), the radial peaking factor was 1.75 and the axial peaking factor was 1.355.

$$f_R(z_P) = \frac{2.405 \cdot R}{2\tilde{R} \cdot J_1 \left(\frac{2.405R}{\tilde{R}} \right)} \tag{2}$$

$$f_A(z_P) = \frac{\pi H}{2\tilde{H} \sin \left(\frac{\pi}{2} \cdot \frac{H}{\tilde{H}} \right)} \tag{3}$$

With these values, the average and hot channel of the fuel rod were deduced using Eq.(4) and Eq.(5) respectively.

Average channel:

$$q_{\text{cell}}(z) = q_{cellAve} \times f_A \times \cos\left(\pi z/\tilde{H}\right) \tag{4}$$

Hot channel:

$$q_{\text{cell}}(z) = q_{cellAve} \times f_A \times f_R \times \cos\left(\pi z/\tilde{H}\right) \tag{5}$$

where z is the cell distance along the height of the fuel rod.

To calculate the enthalpy distribution along the height of the fuel rod (axially), energy balance in the axial location was applied as shown in Eq. (6).

$$i[j] = i[j-1] + \frac{q_{cell}[j-1]}{W} \tag{6}$$

where $[j]$ is the axial cell index along the height of the fuel rod and W is the flow rate.

In calculating the pressure drop along the channel (average and hot) the inlet orifice pressure drop is applied with an unknown orifice local loss coefficient to get about 25% total pressure drop in the core just at the inlet orifice. Therefore, Eqs. (7)- (8) were used to obtain the unknown orifice local loss coefficient (which is a constant) for use in the calculation of the local pressure drop.

$$\Delta p = p_{\text{out}} - p_{\text{in}} = \Delta p_{\text{FuelChannel}} + \Delta p_{\text{Orifice}} \tag{7}$$

$$|\Delta p_{\text{Orifice}}| = \xi_{\text{Orifice}} \frac{G^2}{2\rho} \tag{8}$$

where ξ_{Orifice} is the orifice local loss coefficient, G is the mass flux and ρ is the density.

The total pressure drop along the rod channel is determined by the friction, local, gravity and acceleration (in the case of a two-phase flow) pressure drops along the channel height, as shown in Eq.9.

$$-\Delta p_{\text{tot}} = -\Delta p_{\text{fric}} - \Delta p_{\text{loc}} - \Delta p_{\text{elev}} - \Delta p_{\text{acc}} \tag{9}$$

The pressure drops for a single phase and a two-phase vary and is governed by the condition that the fluid has either exceeded saturation or not. if the fluid is not saturated (that is the quality $x_{eq} < 0$) the flow is single phase, and when the fluid exceeds saturation (that is the quality $x_{eq} \geq 0$) the flow is in two-phase. The pressure drop equations are tabulated in Table.3 with respect to the type of flow.

Table 3: Pressure drop calculation conditions.

Pressure drop	Single phase	Two phase
	$x_{eq} < 0$	$x_{eq} \geq 0$
$-\Delta p_{\text{fric}}$	$\frac{4C_{f,lo}H}{D_h}\frac{G^2}{2\rho_f}$	$\frac{4C_{f,tp}H}{D_h}\frac{G^2}{2\rho_m}$
$-\Delta p_{\text{loc}}$	$\sum_i \xi_i \frac{G^2}{2\rho_f}$	$\sum_i \xi_i \frac{G^2}{2\rho_m}$
$-\Delta p_{\text{elev}}$	$L\rho_f g \sin\varphi$	$L\rho_m g \sin\varphi$
$-\Delta p_{\text{acc}}$	0	$G^2 \left[\frac{1}{\rho_g} - \frac{1}{\rho_f}\right] x_{eq}$

where

$$\rho_m = \frac{\rho_f}{x_{eq}\left(\frac{\rho_f}{\rho_g}-1\right)+1} \qquad \bigg| \qquad \frac{1}{\mu_m} = \frac{x_{eq}}{\mu_g} + \frac{1-x_{eq}}{\mu_f}$$

$$\xi_i = \xi_{in} + \xi_{orifice} + \xi_{spacer} + \xi_{out}$$

The friction coefficient in turbulent flow was calculated using the Haaland formula in Eq.10

$$\frac{1}{\sqrt{C_f}} = -3.6 \log_{10}\left[\left(\frac{k/D_h}{3.7}\right)^{1.11} + \frac{6.9}{\text{Re}}\right] \tag{10}$$

where

$$D_H = D_h = d_r \left[\frac{4}{\pi}\left(\frac{p}{d_r}\right)^2 - 1\right] \quad \bigg| \quad Re = \frac{GD_h}{\mu} \quad \bigg| \quad k = \text{clad roughness}$$

The temperature distribution along the height of the fuel rod (axially) was determined using xsteam, as expressed in Eq.(11). Because they are determinants of the cell location of the fuel rod, the enthalpy and pressure along the height of the rod are not constant.

$$T[j] = xsteam.T\_ph(p[j], i[j]) \tag{11}$$

where p[j] is the pressure and i[j] is the enthalpy at the axial cell location.
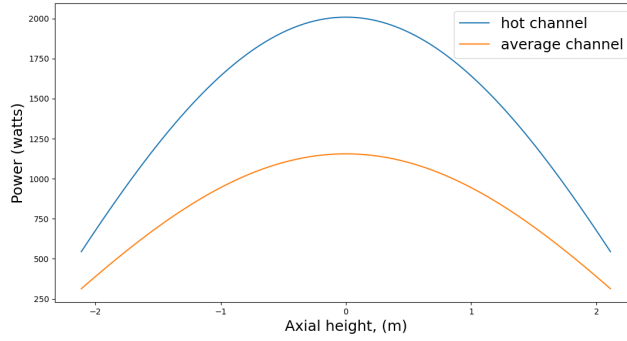
5.3 Results

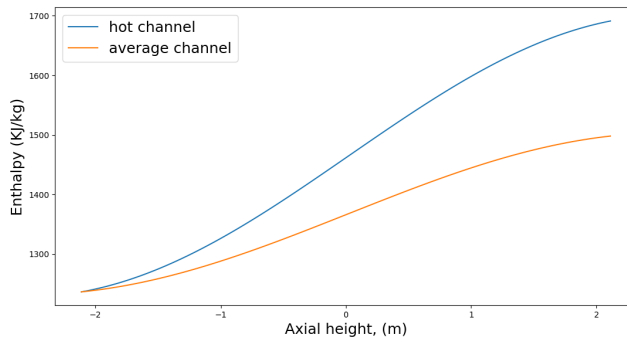Figure 9: Axial power distribution of the average and hot channel.

Figure 10: Axial coolant enthalpy distribution of the average and hot channel.
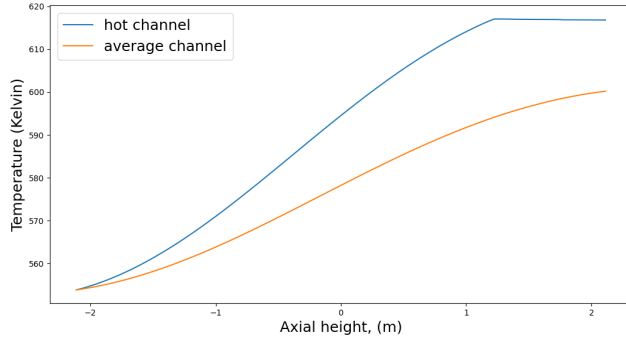
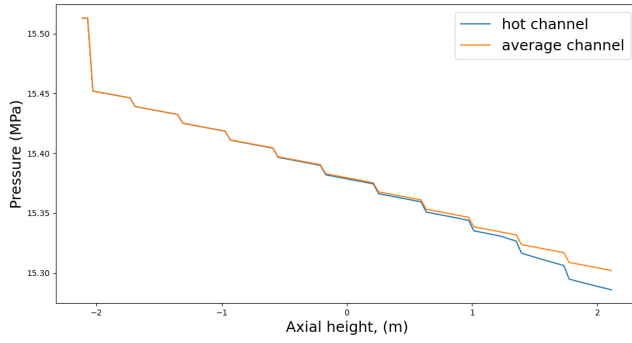Figure 11: Axial temperature distribution of the average and hot channel.

Figure 12: Axial pressure distribution of the average and hot channel.

As shown in Fig. 12, the pressre drop in the hot channel is slightly higher than that in the average channel. This difference is pronounced in the acceleration pressure drop as seen in Fig.13.
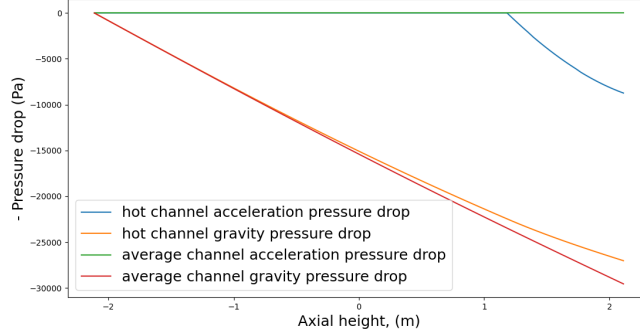
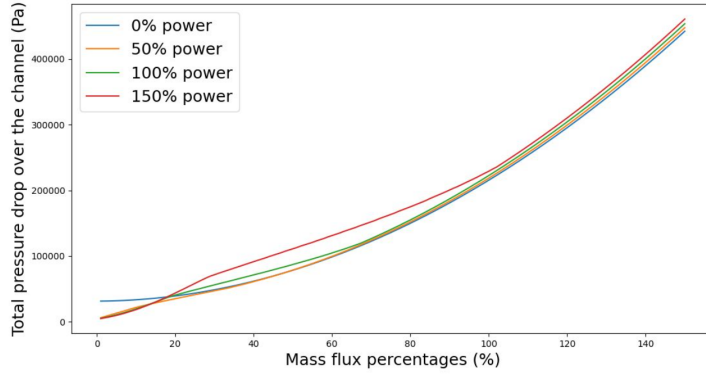Figure 13: Pressure drop along the average and hot channel.

Figure 14: Flow characteristics in the average channel.

5.4   Discussion and Conclusion

Figs. 9-14 shows that reactor properties for the average channel remain in single phase along the channel, while for the hot channel at position 3.36 m on the channel, gets to two-phase.

When we examined the flow characteristics for each power level, we noticed that for 150%, 100%, and 50% power in Fig.14, there was single-phase steam at very low flow rate percentages. Then in the medium flow rate percentages, we noticed that there was 2 phase flow. The transition from single-phase steam to 2 phase flow was marked by a distinct upward bump where the curve shifts from steeper to less steep ascent. In the high flow rate percentages, we noticed that there was single-phase water. The transition from 2 phase flow to single-phase water was also marked by a distinct bump, but this time downward. It occurred

when the curve shifted from a less steep to a steeper ascent. However, for 0% power, since there was no power being produced, there was no heat energy to heat the water. So, there was no single-phase steam or 2 phase flow. Therefore, the flow characteristic for 0% power was a continuous curve representing single-phase water at all flow percentages.

An interesting thing we noted was that, at the very low flow percentages, the total pressure was higher for 0% power than all the other power percentages. This occurred because there was single-phase water at those low flow percentages for 0% power but single-phase steam for the other power percentages. So, the gravity pressure drop and the friction pressure drop at 0% power were higher than those at higher power percentages. That is why the total pressure drop was higher for 0% power at the lowest flow percentages.

AP1000 is designed not to boil, meaning two-phase is not possible in a real design. However, in this claculation it is seen that the hot channel gets to two-phase towards the top tail of the channel. I reckon this phenomena is possible because the hot channel is not a realistic channel (given that it includes both radial and axial peaking factors at the same time at the same rate). With this model the rated power without two-phase was deduced at 83% of the norminal power.

6 Task 5: Calculation of CHF margins in a hot channel

6.1 Introduction

CHF (Critical Heat Flux) is one of the factors that limit the maximum thermal power in the core. In this task, the margin of CHF occurrence is estimated using the hot channel. The calculation was estimated at normal operating power and also at instances when the power was increased while keeping all other parameters constant until the CHF condition was achieved. The objective is to plot the axial distribution of departure from nucleate boiling ratio (DNBR) and the axial location of the minimum DNBR.

6.2 Methods

To determine the margin of CHF occurrence in the hot channel, the minimum nucleate boiling ratio is determined using the expression below

$$MDNBR = \frac{\text{minimum critical heat flux in hot channel } q''_{cr}(z)}{\text{local actual heat flux in hot channel } q''(z)}$$

The local actual heat flux is calculated using the power initially calculated using (Eq. (5)) for the hot channel. And the critical quality was determined

using the Reddy Fighetti Subchannel CHF correlation in Eq.(12).

$$q''_{cr}(\mathbf{r}) = B \frac{A - x_{in}}{C + \frac{x(\mathbf{r}) - x_{in}}{q''_R(\mathbf{r})}} \tag{12}$$

where A, B and C are constants and x_{in} is the inlet enthalpy. The applicable range of the correlation is as follows:

$\mathbf{147 < G < 3023}$ kg/m$\mathbf{^2}$ s	$\mathbf{-0.25 < x < 0.75}$	$-1.10 < x_{in} <= 0.0$
$0.762 < L < 4.267$ m	$6.3 < D_H <= 13.9$ mm	$13.8 < P <= 169.9$ bar

6.3 Results

In this subsection, the MDNBR was deduced at 100% and 161% norminal power in the hot channel.
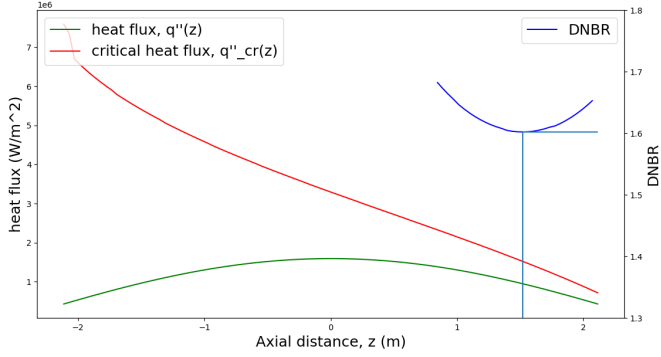

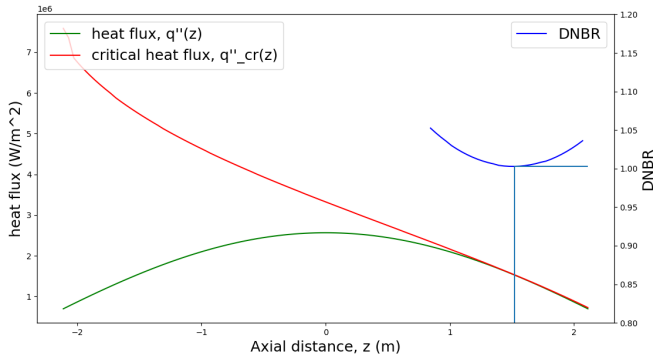Figure 15: DNBR at 100% power in the hot channel.

Figure 16: DNBR at 161% power in the hot channel.

6.4   Discussion and Conclusion

As seen in Fig. 15,the CHF have not been exceeded at norminal power and the MDNBR value is 1.602, but at the power is increased to 161% of the norminal power, the MDNR value gets 1.009. Acording to [18] the minimum DNBR at norminal conditions for AP1000 at a typical flow channel is 2.80 and at design transients it is ¿1.25¡1.22. Also in refrence to [19] the minimum value of DNBR for design purposes in PWR reactors should be 1.3. Therefore, it can be deduced that the hot channel at norminal power has not reached CHF. It has gotten to nucleate boiling since the channel flow is in two-phase, but it has not departed from nucleate boiling.

7   Task 6: Calculation of the maximum cladding and fuel pellet temperature

7.1   Introduction

In this task, the maximum cladding and fuel pellet temperatures were calculated and the locations of the hot spots were identified. Again the calculations were based on AP1000 parameters tabulated in table 2.

7.2   Methods

In estimating the radial distribution of the fuel rod's temperature in the hot channel. The change in temperature was determined by working inwards from the coolant temperature to the centre of the fuel pellet. Due to the variable composition of the fuel rod, it was necessary to determine the temperature difference between the cladding, the gap, and the fuel pellet. Fig.17: depicts a radial diagram illustrating the approach.
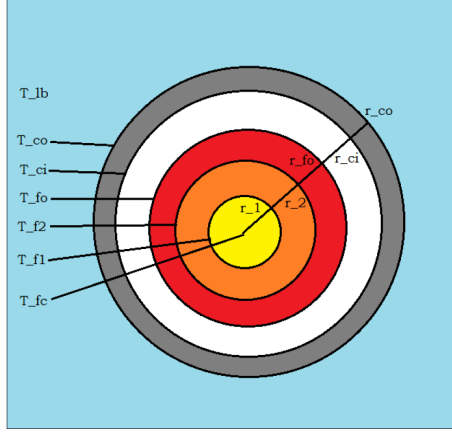
Figure 17: Radial temperature calculation model.

Given that T_{lb} the coolant temperature for the hot channel has already been calculated in subsection 5.3, the cladding temperature T_{co} is deduced using Eqs. (13) - (16)

$$T_{co} = T_{lb} + \Delta T_{lb}, \tag{13}$$

$$\Delta T_{lb} = \frac{q''}{h}, \tag{14}$$

$$h = \frac{Nu\lambda_l}{D_h}, \tag{15}$$

where h is the heat transfer coefficient of the coolant.

$$Nu = 0.023 \times Re^{0.8} \times Pr^{0.4}, \tag{16}$$

where Nu is the Nusselt number given by Dittus Boelter, the Prandtl number is expressed as $Pr = \frac{C_p\mu}{\lambda_l}$, and the Reynolds number is expressed as $Re = \frac{GD_h}{\mu}$.

From subsection 5.3 results, it is evident that two-phase occurs towards the end of the hot channel, and given that, the Dittus Boelter's correlation is only viable in single phase. The chen correlation Fig.18 was used to determine the heat transfer coefficient (h).
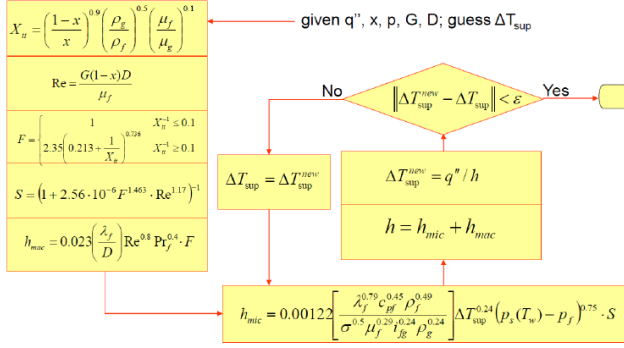
Figure 18: Chen Correlation.

Eq.(17) was used to determine the temperature difference at the cladding by iteratively calculating the thermal conductivity of the cladding as shown in Fig.19.

$$\Delta T_C = \frac{q''' r_{fo}^2}{2\lambda_C} \ln\left(\frac{r_{co}}{r_{ci}}\right),\tag{17}$$
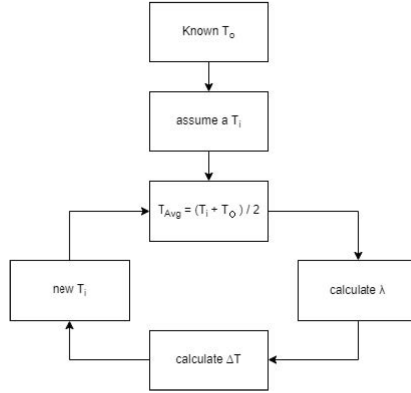
where $\lambda_C = 12.6 + 0.0118T$.

Figure 19: Iterative scheme to find λ.

Eq.(18) was used to determine the temperature difference at the gap.

$$\Delta T_G = \frac{q''' r_{fo}^2}{2\lambda_G} \ln\left(\frac{r_{ci}}{r_{fo}}\right),\tag{18}$$

where λ_G was assumed to be 0.6W/mK.

24

Eq.(19) was used to determine the temperature difference in the fuel by iteratively calculating the thermal conductivity of the fuel as illustrated in Fig.19. As seen in Fig.17 the pellet was divided into three regions to accurately deduce the temperature at the centre.

$$\Delta T_F = \frac{q'''(z)\left(r^2_{\text{F, cell o}} - r^2_{\text{F, cell i}}\right)}{4\lambda_F},$$ (19)

where $t = T/1000$ and $\lambda_F = \frac{100}{7.5408+17.692t+3.6142t^2} + \frac{6400}{t^{5/2}}\exp\left(-\frac{16.35}{t}\right)$.

7.3 Results

Figs.20-21 represents the temperature distribution along the rod height in the coolant, gap, cladding and fuel pellet. Temperatures in the coolant, gap, and cladding were found to have a comparable form along the rod height, as opposed to temperature in the fuel, which resembled the axial power distribution along the height.
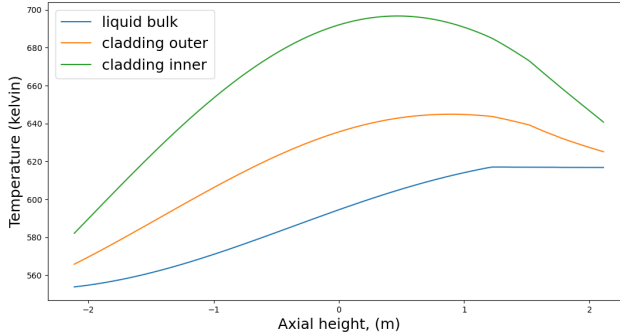

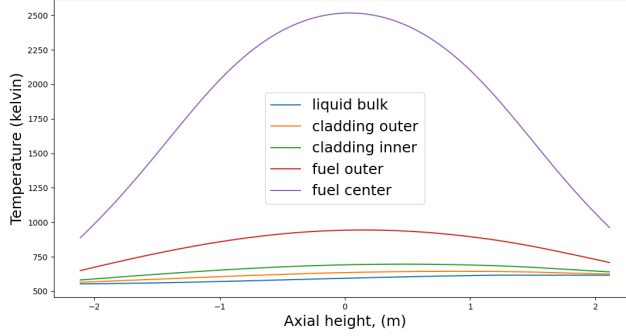Figure 20: Temperature in fuel pellet.

Figure 21: Temperature distribution along the axial channel.

The radial temperature distribution from the maximum location in the channel is shown in Fig.22, and as observed, a transition between the calculation from the cladding, gap, and fuel to the fuel centre line is pronounced with changes in the plot distribution form at specific locations.
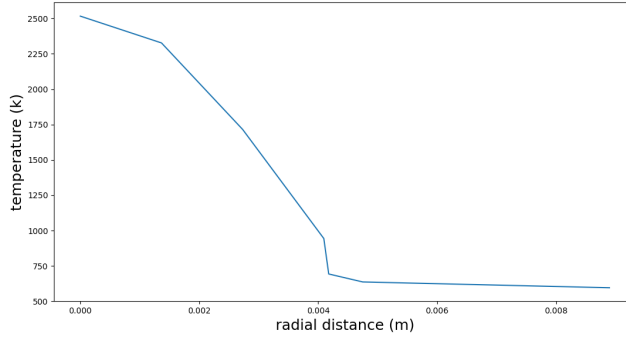

Figure 22: Radial temperature distribution at z = 0 m.

7.4   Discussion and Conclusion

The graph plotted in Fig.22 demonstrates that the maximum fuel temperature is 2516 K at 2.18 m of the fuel rod's height, and the maximum cladding temperature deduced from Fig.20 is 697 K at 2.6 m of the fuel rod's height. According to [3], the melting temperature of AP1000 fuel is 3078 K while the maximum allowable temperature in the cladding is 1477 K. These values show that the maximum allowable temperature in the cladding and the melting temperature of the fuel were not exceeded in these calculations.

References

[1] Westinghouse, "Status report 81-Advanced Passive PWR (AP 1000)," Tech. Rep., 2011.

[2] Westignhouse, "AP1000 Deign Control Document: CHAPTER 4 REACTOR 4.1 Summary Description," Tech. Rep., 2011.

[3] G. Laranjo de Stefani, J. Rubens Maiorino, G. Laranjo Stefani, P. R. Rossi, J. R. Maiorino, and T. A. Santos, *NEUTRONIC AND THERMAL-HYDRAULIC CALCULATIONS FOR THE AP-1000 NPP WITH THE MCNP6 AND SERPENT CODES*, 2015. [Online]. Available: https://www.researchgate.net/publication/288667236

[4] T. L. Schulz, "Westinghouse AP1000 advanced passive plant," *Nuclear Engineering and Design*, vol. 236, no. 14-16, pp. 1547–1557, 8 2006.

[5] Wikipedia, "Balance of plant." [Online]. Available: https://en.wikipedia.org/wiki/Balance_of_plant

[6] S. Cullen, "Evaluating Nuclear Power Stations as a Viable Replacement for Moneypoint Power Station, Ireland," 2017. [Online]. Available: https://www.researchgate.net/publication/340829872

[7] Westinghouse Electric Company LLC, "AP1000 Pre-Construction Safety Report," Tech. Rep., 2017.

[8] M. Onoue, T. Kawanishi, W. R. Carlson, and T. Morita, "Application of MSHIM Core Control Strategy For Westinghouse AP1000 Nuclear Power Plant," Tech. Rep., 2003.

[9] Westinghouse, "AP1000 Design Control Document: Chapter 7: Control and Instrumentation Systems," 2011.

[10] ——, "CHAPTER 15 Accident Analyses AP1000 Design Control Document," Tech. Rep., 2011.

[11] US Nuclear Regulatory Commission, "NUREG-2194, Vol. 1, "Standard Technical Specifications Westinghouse Advanced Passive 1000 (AP1000) Plants."," Tech. Rep., 2016. [Online]. Available: www.nrc.gov/reading-rm.html.

[12] M. Hashim, H. Yoshikawa, T. Matsuoka, and M. Yang, "Quantitative dynamic reliability evaluation of AP1000 passive safety systems by using FMEA and GO-FLOW methodology," *http://dx.doi.org/10.1080/00223131.2014.881727*, vol. 51, no. 4, pp. 526–542, 4 2014. [Online]. Available: https://www.tandfonline.com/doi/abs/10.1080/00223131.2014.881727

[13] P. Gaio, "AP1000 The PWR Revisited," Tech. Rep.

[14] R. Schène, "The Westinghouse Advanced Passive Pressurized Water Reactor, AP1000 TM," Tech. Rep., 2009.

[15] US Nuclear Regulatory Commission, "NUREG-2194, Vol. 2, "Standard Technical Specifications Westinghouse Advanced Passive 1000 (AP1000) Plants. Volume 2: Bases."," Tech. Rep., 2016. [Online]. Available: www.nrc.gov/reading-rm.html.

[16] Westinghouse, "AP 1000 Design Control Document: Introduction and General Description of the Plant," Tech. Rep., 2011.

[17] "ARIS - Technical Data." [Online]. Available: https://aris.iaea.org/sites/RCS.html

[18] Westinghouse, "AP1000 Deign Control Document: Chapter 4. 4 Reactor," Tech. Rep., 2011.

[19] Lamarsh and Baratta, "Introcution to Nuclear Engineering," *Prentice hall*, vol. 3rd editio, pp. 1–783, 2001.